



Published in final edited form as:

*J Immunol.* 2011 July 1; 187(1): 450–461. doi:10.4049/jimmunol.1000964.

## FIZZ2/RELM- $\beta$ Induction and Role in Pulmonary Fibrosis

Tianju Liu<sup>\*,1</sup>, Hyun Ah Baek<sup>†,1</sup>, Hongfeng Yu<sup>\*</sup>, Ho Jin Lee<sup>†</sup>, Byung-Hyun Park<sup>‡</sup>, Matthew Ullenbruch<sup>\*</sup>, Jianhua Liu<sup>\*</sup>, Taku Nakashima<sup>\*</sup>, Yoon Young Choi<sup>\*</sup>, Gary D. Wu<sup>§</sup>, Myoung Ja Chung<sup>†</sup>, and Sem H. Phan<sup>\*</sup>

<sup>\*</sup>Department of Pathology, University of Michigan Medical School, Ann Arbor, MI 48109

<sup>†</sup>Department of Pathology, Chonbuk National University Medical School, Jeonju 561-180, Korea

<sup>‡</sup>Department of Biochemistry, Chonbuk National University Medical School, Jeonju 561-180, Korea

<sup>§</sup>Division of Gastroenterology, University of Pennsylvania, Philadelphia, PA 19104

### Abstract

Found in inflammatory zone (FIZZ) 2, also known as resistin-like molecule (RELM)- $\beta$ , belongs to a novel cysteine-rich secreted protein family named FIZZ/RELM. Its function is unclear, but a closely related family member, FIZZ1, has profibrotic activities. The human ortholog of rodent FIZZ1 has not been identified, but human FIZZ2 has significant sequence homology to both rodent FIZZ2 (59%) and FIZZ1 (50%). Given the greater homology to rodent FIZZ2, analyzing the role of FIZZ2 in a rodent model of bleomycin-induced pulmonary fibrosis would be of greater potential relevance to human fibrotic lung disease. The results showed that FIZZ2 was highly induced in lungs of rodents with bleomycin-induced pulmonary fibrosis and of human patients with idiopathic pulmonary fibrosis. FIZZ2 expression was induced in rodent and human lung epithelial cells by Th2 cytokines, which was mediated via STAT6 signaling. The FIZZ2 induction in murine lungs was found to be essential for pulmonary fibrosis, as FIZZ2 deficiency significantly suppressed pulmonary fibrosis and associated enhanced extracellular matrix and cytokine gene expression. In vitro analysis indicated that FIZZ2 could stimulate type I collagen and  $\alpha$ -smooth muscle actin expression in lung fibroblasts. Furthermore, FIZZ2 was shown to have chemoattractant activity for bone marrow (BM) cells, especially BM-derived CD11c<sup>+</sup> dendritic cells. Notably, lung recruitment of BM-derived cells was impaired in FIZZ2 knockout mice. These findings suggest that FIZZ2 is a Th2-associated multifunctional mediator with potentially important roles in the pathogenesis of fibrotic lung diseases.

---

Copyright © 2011 by The American Association of Immunologists, Inc.

Address correspondence and reprint requests to Dr. Myoung Ja Chung or Dr. Sem H. Phan, Department of Pathology, Chonbuk National University Medical School, Jeonju 561-180, Korea (M.J.C.) or Department of Pathology, University of Michigan Medical School, 109 Zina Pitcher Place, Ann Arbor, MI 48109 (S.H.P.). mjchung@jbnu.ac.kr (M.J.C.) or shphan@umich.edu (S.H.P.).

<sup>1</sup>T.L. and H.A.B. contributed equally to this work.

The microarray data presented in this article have been submitted to the Gene Expression Omnibus database under accession number GSE25640.

### Disclosures

The authors have no financial conflicts of interest.

Many of the interstitial lung diseases develop pulmonary fibrosis, which may progress to end-stage lung disease. In certain subtypes, such as idiopathic pulmonary fibrosis, there is currently no proven effective treatment (1, 2). Additionally, certain airway diseases, such as asthma, involve significant degree of tissue remodeling or fibrosis (3, 4). The observed fibrosis in these diseases exhibits certain common features, such as extracellular matrix deposition and the involvement of myofibroblasts and Th2 cytokines (5–8). Many of the features found in these fibrotic lung diseases can be recapitulated in studies of pulmonary fibrosis using animal models, albeit not all can be faithfully reproduced in any one animal model. The bleomycin-induced model used in this study models certain aspects of the fibrotic response in the lung in these various human interstitial lung diseases with fibrosis affecting the distal lung parenchyma. Despite extensive research efforts including the use of such animal models, the precise mechanism underlying the development of many of these diseases, including especially idiopathic pulmonary fibrosis (IPF), remains elusive, and no effective therapy yet exists (1, 2). Although an expanding list of potentially important mediators, such as cytokines, have been identified from these studies, it is clear from the failures of many clinical trials targeting the known ones that the entire spectrum of important mediators and genes have yet to be identified. The hallmark lesions of chronic fibrotic lung diseases are increased number of fibroblasts, de novo emergence and persistence of myofibroblasts, as well as the deposition of extracellular matrix (5–7). It is postulated that cytokines and chemokines such as TGF- $\beta$  produced by repeatedly injured alveolar epithelial cells recruit adjacent underlying fibroblasts to constitute so-called fibroblast foci composed of fibroblast-like cells, including myofibroblasts (1, 9). In addition to TGF- $\beta$ , a recently identified novel mediator, found in inflammatory zone (FIZZ) 1, also known as resistin-like molecule (RELM)- $\alpha$ , is also a known inducer of myofibroblast differentiation in rodents (10, 11). FIZZ1 is primarily expressed by airway and alveolar epithelial cells (AECs), which is driven by the Th2-type cytokines IL-4 and IL-13. It has a direct profibrogenic activity by its ability to stimulate type I collagen and  $\alpha$ -smooth muscle actin ( $\alpha$ -SMA) expression in lung fibroblasts, which is mediated by Jagged1/Notch1 signaling (11–13). Moreover, FIZZ1 has protective effects against lung fibroblast apoptosis mediated by the ERK pathway, which may prolong survival and persistence of myofibroblasts (14). These properties indicate that FIZZ1 may play a pivotal role in mediating the cross-talk between epithelial and fibrotic cells that is assumed as being important in formation of fibroblast foci and persistence as well as progression of fibrosis (11–13). However, the potential relevance of these fibrogenic activities of rodent FIZZ1 to human fibrotic lung disease is unknown and unexplored because the human ortholog of FIZZ1 has not been identified (15). However the human ortholog of a closely related member, FIZZ2, has been identified.

As the name suggests, FIZZ2 is also a member of the FIZZ/RELM family, which is known currently to consist of four members: FIZZ1/RELM- $\alpha$ , FIZZ2/RELM- $\beta$ , FIZZ3/resistin, and RELM- $\gamma$  (16). This cysteine-rich secreted protein family is characterized by their conserved 10 cysteine residue motif, with two members, FIZZ2 and resistin, having an additional cysteine residue in the highly variable N terminus. The FIZZ family has a unique tissue expression pattern. FIZZ1, initially found in lung allergic inflammation, is expressed predominately in white adipose tissue with low levels of expression noted in lung, heart, and

mammary glands. FIZZ2 is specifically expressed by goblet cells and epithelial cells mainly in gastrointestinal tract, and recently found in airway epithelium as well, but not in white adipose tissue where FIZZ3 is exclusively expressed (15, 17, 18). FIZZ2 is involved in pathogenesis of glucose tolerance and hyperlipidemia in some insulin-resistant models, such as obesity and fatty liver (19, 20). Additionally, FIZZ2 is reported to have a role in the maintenance of gastrointestinal barrier function and promotes resistance to gastrointestinal nematode infection (21, 22).

Whereas rodent FIZZ1 has a profibrogenic activity in rodent pulmonary fibrosis through both induction of myofibroblast differentiation and prolonged survival of myofibroblasts (11, 14), FIZZ2 is shown to have a role in promoting airway inflammation and remodeling in a murine model of allergic airway disease (18). But this previous study does not examine its role in parenchymal or interstitial fibrosis affecting areas distal to the major airways. Recent reports suggest the possibility that human FIZZ2 may represent the human ortholog of rodent FIZZ1, especially at the functional level (23). However, given that 1) the human ortholog of rodent FIZZ1 has yet to be unequivocally identified and 2) human FIZZ2 is more homologous to rodent FIZZ2 than FIZZ1 (59 versus 50%) (17), studies of rodent FIZZ2 are necessary to provide insight of greater relevance to human fibrotic lung disease. FIZZ2 is upregulated by hypoxia in a human A549 lung epithelial cell line, and its overexpression induces significant proliferation in these cells, suggesting a potential role in hypoxia-induced pulmonary disease and associated vascular remodeling (23). More recent evidence reveals that FIZZ2 expression is significantly increased in human lungs from patients with pulmonary fibrosis, asthma, and pulmonary hypertension (18, 24, 25). Notably, the chromosome locus of human FIZZ2 gene (3q13.1) has recently been linked to allergic inflammation (26).

The objective of the current study was to investigate the role of FIZZ2 in pulmonary fibrosis in a rodent bleomycin (BLM) model and also explore the potential relevance to the role of human FIZZ2 in human fibrotic lung disease. The results showed that FIZZ2 is highly induced in fibrotic rodent as well as human lung, and its deficiency in mice significantly impaired BLM-induced fibrosis. Analysis of its biological activity revealed multiple potential roles in pathogenesis of pulmonary fibrosis, including stimulation of fibroblast proliferation, promotion of myofibroblast differentiation, and the recruitment of bone marrow-derived cells to the lung.

## Materials and Methods

### Animals and induction of pulmonary fibrosis

Six-week-old female CBA/J, C57BL/6, BALB/c, and GFP transgenic mice on C57BL/6 background mice were purchased from The Jackson Laboratory (Bar Harbor, ME), and 7~8-wk-old female Fisher 344 rats were purchased from Charles River Breeding Laboratories (Wilmington, MA). FIZZ2 knockout (KO) mice on C57BL/6 background were generated as previously described (27). These FIZZ2 KO mice were propagated at the University of Michigan, and progeny exhibited no gross anatomic abnormalities. IL-4 KO mice and IL-4/IL-13 double KO mice were kindly provided by Dr. Andrew McKenzie (Medical Research Council Laboratory of Molecular Biology, University of Cambridge, Cambridge, U.K.) (28).

STAT6 KO mice were kindly provided by Nicholas Lukacs (University of Michigan, Ann Arbor, MI) and derived from mice developed by Mark H. Kaplan (Indiana University School of Medicine, Indianapolis, IN) (29). Pulmonary fibrosis was induced by the endotracheal injection of 7.5 U/kg body weight BLM (Blenoxane; Mead Johnson, Plainsboro, NJ) into rats, 2 U/kg into C57BL/6 mice, or 10 U/kg into BALB/c mice, as described previously (6). The control group received the same volume of sterile PBS only. At 7, 14, or 21 d after BLM injection, the animals were sacrificed and the lungs were removed for mRNA and protein analysis or used for isolation of fibroblasts. In some experiments, lungs were fixed with 10% neutral buffered formalin for immunohistochemistry. Where indicated, bronchoalveolar lavage fluid (BALF) was collected by lavaging the lung five times with 1 ml PBS each time. Bronchoalveolar lavage (BAL) cells were pelleted by centrifuging BALF at  $400 \times g$  for 10 min and resuspended in PBS. Total cell number was counted using a hemocytometer. BAL cells were then subjected to flow cytometry for differential analysis. Whole-lung single-cell suspension was produced by mincing and digesting the lungs with collagenase III (Worthington Biochemical Corp., Lakewood, NJ), and then followed by flow cytometry for CD3 T cell analysis. For histopathologic analysis, 21 d after BLM injection, the lungs were formalin-fixed and stained with H&E.

GFP-bone marrow (BM) chimeras were generated by transplantation of BM cells from GFP transgenic mice to lethally irradiated wild-type (WT) or FIZZ2 KO recipient mice as previously described (30). Six weeks after transplantation, pulmonary fibrosis was induced by endotracheal BLM injection as described earlier. Twenty-one days after BLM injection, the lungs were removed for analysis of BM cell recruitment to the lung.

### Cell isolation and functional analysis

Rat AECs were isolated by elastase digestion and IgG panning as previously described (31). The cells were suspended in DMEM supplemented with 10% FBS (Sigma-Aldrich, St. Louis, MO) and then plated onto 6-well tissue culture plates precoated with fibronectin (R&D Systems, Minneapolis, MN). Isolated cells were consistently 90% epithelial cells as evaluated by immunostaining with anti-cytokeratin 5/8 Abs (BD Biosciences, San Diego, CA), which recognized the cytokeratins found in AECs but not present in macrophages, fibroblasts, or endothelial cells (31). Human primary small airway epithelial cells (PCS-301-010) were purchased from American Type Culture Collection (Manassas, VA). To evaluate regulation of FIZZ2 expression, both rodent and human epithelial cells at ~90% confluence were made quiescent by culturing for 4–6 h in DMEM containing 0.5% FBS for rat AECs, or in airway epithelial cell basal medium containing 1% bronchial epithelial cell growth kit (American Type Culture Collection) for human small airway epithelial cells. Where indicated, 10 ng/ml each of rIL-4, rIL-13, rIL-17, or IFN- $\gamma$  (R&D Systems) was then added, and the cells were further incubated for 4 or 8 h before harvesting for total RNA isolation.

Mouse lung fibroblasts (MLFs) were isolated from the indicated murine strain and maintained in culture as described previously (6). Fibroblasts between passages 3 and 5 after primary culture were used unless otherwise specified. Where indicated, recombinant mouse

FIZZ2 (Leinco Technologies, St. Louis, MO) and/or TGF- $\beta$ 1 (R&D Systems) were added to the medium at the indicated concentrations and time points to analyze their effects on fibroblast function.

### mRNA analysis by quantitative PCR or regular RT-PCR

Total RNA was isolated from lung tissue, lung fibroblasts, and AECs after indicated treatments. Primer Express 2.0 software (Applied Biosystems, Foster City, CA) was used to design TaqMan primers, and MGB probes (6-FAM conjugated) for FIZZ2 and  $\alpha$ -SMA were then purchased from Applied Biosystems. The following oligonucleotide primers and probes were used: rat FIZZ2 sense (5'-CATGAAGCCTACACTGTGTTTCCTT-3') and antisense (5'-TGGGACCATCAGCGAGAG-3'), and probe (FAM) (5'-TCATCCTCATCTTCC-3'); mouse FIZZ2 sense (5'-GGGATGGTTGTCACCTGGATGT-3') and antisense (5'-CACTGGCAGTGGCAAGTATTTC-3'), probe (FAM) (5'-TGGCTATGGCTGTGGATCGTGGG-3'); mouse  $\alpha$ -SMA sense (5'-CTGGAGAAGAGCTACGAACTGC-3') and antisense (5'-CTGATCCACATCTGCTGGAAGG-3'), and probe (FAM) (5'-CTGACGGGCAGGTGA-3'). Primers and probes for mouse type I collagen, MCP-1, TERT, IL-4, FIZZ3, RELM- $\gamma$ , and GAPDH were purchased from Applied Biosystems. Real-time quantitative PCR (qPCR) was performed on a TaqMan ABI 5700 Sequence Detection System (Applied Biosystems). For each assay, 100 ng total RNA was used as template. The mRNA levels were normalized to GAPDH signal.

Three-step cycling RT-PCR for FIZZ2 mRNA was performed using Superscript One-Step RT-PCR with platinum Taq kit (Invitrogen, Carlsbad, CA). Primer sequences used for mouse FIZZ2 were as follows: mouse FIZZ2 sense (5'-CGCAATGCTCCTTTGAGTCT-3') and antisense (5'-GGATATCCCACGATCCACAG-3'). Two micrograms of total RNA for each sample was used in the cDNA synthesis.

### Immunohistochemistry for FIZZ2

Lung tissues from patients with IPF or nonspecific interstitial pneumonia (NSIP) were obtained through the Biobank of Chonbuk National University Hospital, a branch of National Biobank of Korea. Subjects included in this study satisfied the American Thoracic Society/European Respiratory Society criteria for IPF or NSIP. For comparison, normal lung tissue from resected specimens for lung cancer was included. Rodent lung tissue samples were obtained as described earlier. Formalin-fixed paraffin-embedded tissue sections were deparaffinized in xylene and rehydrated in graded alcohols. Ag retrieval was achieved by incubating tissue sections in boiling 10 mmol/l citrate buffer (pH 6), and immunostaining was undertaken using primary Ab against FIZZ2 (Sigma). Biotin-conjugated secondary Ab and streptavidin solution were used to develop color with 3-amino-9-ethylcarbazole (Lab Vision, Fremont, CA) as a chromogen.

### Western blotting analysis

Total protein was isolated from cultured MLFs and snap-frozen mouse lung tissues using lysis buffer (50 mM Tris HCl, pH 7.5, 1% Nonidet P-40). Equal amount of protein was loaded onto SDS-PAGE gels for separation and transferred to nitrocellulose membrane for immunoblotting. The following Abs were used: anti FIZZ2, anti- $\alpha$ -SMA (Sigma), anti-

collagen type I (Bioscience International, Saco, ME), anti-phospho-ERK, anti-phospho-AKT, anti-phospho-JNK, or anti-phospho-p38 (Cell Signaling Technology, Danvers, MA).

### Fibroblast proliferation assay

Cell proliferation was evaluated using the tetrazolium salt [3-(4,5-dimethylthiazol-2-yl)-5-(3-carboxymethoxyphenyl)-2-(4-sulfophenyl)-2H-tetrazolium; inner salt] (MTS), which is cleaved to formazan in metabolically active cells. Briefly, MLFs ( $4 \times 10^4$ ) were seeded into 96-well plates. After incubation for 24 h, cells were starved for 24 h with DMEM containing 0.5% FBS. FIZZ2 at the indicated concentrations was then added into the wells. Cell proliferation was evaluated after 1 d of treatment. In some experiments, the MAPK inhibitor PD98059 was added into cells before FIZZ2 treatment to evaluate ERK dependency on the FIZZ2-mediated fibroblast proliferation. Ten microliters/well MTS was added for 2 h at the end of stimulation. The absorbance of the treated samples against a blank control was measured using a ThermoMax microplate reader (Molecular Devices, Menlo Park, CA) at 450 nm with a reference wavelength of 650 nm.

### Apoptosis assay

MLFs ( $1 \times 10^6$  cells) were plated onto 60-mm plates, and when sub-confluent they were serum deprived in DMEM with 0.5% PDS for 24 h. The antiapoptotic effect of FIZZ2 was studied by treating cells with 10 or 25 ng/ml FIZZ2 for 24 h. To optimize induction of apoptosis of MLFs, cells were treated with 5 ng/ml TNF- $\alpha$  (R&D Systems) and 500 ng/ml cycloheximide with or without FIZZ2 for up to 24 h. Apoptosis was evaluated as before (14) using annexin V-propidium iodide (PI) staining (TACS Annexin V-FITC; R&D Systems) and analyzed by FACSCaliber (BD Biosciences). Apoptotic cells were identified as an annexin V<sup>+</sup>/PI<sup>-</sup> population.

### Hydroxyproline assay

Lung collagen deposition was estimated by measuring the hydroxyproline content of whole-lung homogenates as previously described (32). Briefly, the lungs were excised, homogenized in 0.5 M acetic acid, and hydrolyzed in 6 N HCl overnight at 110°C. Hydroxyproline was assessed by colorimetric assay, and the results were expressed as micrograms hydroxyproline per lung.

### BM cell isolation and migration assay

Mouse and rat BM cells were isolated from femurs and tibias by aspiration and flushing as before (30). Where indicated, bone marrow-derived dendritic cells (BMDCs) were induced with 10 ng/ml GM-CSF (R&D Systems) and purified with the MACS system using CD11c<sup>+</sup> microbeads (Miltenyi Biotec, Auburn, CA). For cell migration assay,  $1 \times 10^6$  BM cells or BMDCs were prestained with a fluorescent dye Calcein AM (BD Biosciences) and then plated into inserts with 5- $\mu$ m pore size in 24-well Transwell Boyden chambers (Fisher Scientific, Waltham, MA). FIZZ2 was added into the lower chamber at the indicated concentration. After 2 h of incubation, fluorescence was read at wavelengths of excitation 494 nm/emission 517 nm using a Spectramax Gemini XS Microplate Spectrofluorometer (Molecular Devices).

## Flow cytometry

The BAL cells were stained with F4/80–Alexa 647 (eBioscience, San Diego, CA), CD3–PE–Cy7 (eBioscience), and Gr-1–PE (eBioscience) conjugated Abs for macrophages, CD3 T cells, and neutrophils, respectively. The lung tissue single-cell suspensions were stained with CD3–PE–Cy7 Ab. Where indicated in BM transplantation experiments, MLFs were isolated from BLM or saline-treated GFP-BM chimera mouse lungs. The primary cultured MLFs without passaging were used for this experiment. The cells were stained with CD11c–PE conjugates (BD Biosciences), and then CD11c<sup>+</sup> and GFP<sup>+</sup> cells were analyzed by FACSCaliber flow cytometry (BD Biosciences).

## Gene microarray analysis

Total RNA isolated from control or FIZZ2-treated MLFs as well as day 7 BLM/saline-treated WT or FIZZ2 KO murine lungs were used for microarray analysis using 30,000-element (30K) mouse Affymetrix oligonucleotide genechips, cRNA labeling and hybridization were performed, and the primary data were obtained using the Affymetrix Microarray Core facility at the University of Michigan (33, 34).

## Statistical analysis

All data were expressed as mean  $\pm$  SE. Differences between means of various treatment groups were assessed for statistical significance by ANOVA followed by post hoc testing using Scheffé's test. A *p* value <0.05 was considered to indicate statistical significance.

## Results

### Induction of FIZZ2 expression in pulmonary fibrosis

To assess initially a potential role for FIZZ2 in pulmonary fibrosis, its expression in lung tissue was examined in both a rodent model and human IPF. Assessment by qPCR revealed undetectable levels of FIZZ2 mRNA in lungs from control (PBS-treated) rats or mice (Table I). However, FIZZ2 mRNA expression was induced and easily detectable in lung tissues of BLM-treated animals as early as 1 wk after BLM treatment (Table I). To confirm the qPCR results, standard RT-PCR and Western blot analyses were undertaken to assess FIZZ2 mRNA and protein expression levels in lung tissues from day 7 BLM-treated and control mice. Confirming the qPCR results, FIZZ2 mRNA was detected only in BLM-treated lung tissue (Fig. 1A). Western blotting results were consistent with the mRNA findings in showing the marked upregulation in lung FIZZ2 protein levels; although unlike the undetectable mRNA in control mice, trace levels of protein were present in the control samples (Fig. 1B). These results indicated that FIZZ2 expression was induced in BLM-induced pulmonary fibrosis. FIZZ3 and RELM- $\gamma$  mRNA levels were also analyzed, and the results showed that unlike FIZZ2, FIZZ3 and RELM- $\gamma$  were not induced in BLM-treated mouse lungs compared with their expressions from their respective saline control groups (Fig. 1C). To localize the cellular sources of induced FIZZ2 expression, immunohistochemistry for FIZZ2 protein was performed in lung tissues from day 14 BLM-/saline-treated mice. As expected, histologically BLM-treated lung showed inflammation, distortion of normal lung architecture, collagen deposition, and epithelial hyperplasia (Fig. 1D). Consistent with the mRNA and protein data, immunohistochemical staining revealed

induction of FIZZ2 expression in BLM-treated lungs, but this was only faintly detectable in a few cells in the control lungs (Fig. 1*Db* and 1*Dd*, respectively). Expression was localized mainly to airway epithelial cells and AECs, in which regeneration and/or hyperplasia was frequently recognized. FIZZ2 was also seen in alveolar macrophages. Weak staining was also observed in some vascular smooth muscle and endothelial cells. There was no detectable signal of FIZZ2 in fibroblasts, which was confirmed by undetectable FIZZ2 mRNA by qPCR in fibroblasts isolated from day 7 BLM-treated or control murine lungs using qPCR (data not shown).

Recent reports indicate upregulated lung FIZZ2 expression in human inflammatory and fibrotic lung diseases, suggesting a potential role in pathogenesis. To determine if this was also the case in human interstitial lung disease, lung tissue specimens from patients with IPF or NSIP were analyzed by immunohistochemistry for FIZZ2 expression. Consistent with the murine lung findings (Fig. 1*D*), normal human lung tissue (from normal margins of resected cancerous lung tissue) exhibited only weak staining for FIZZ2 in scattered isolated alveolar macrophages and a few epithelial cells (Fig. 1*Ed*). In contrast, NSIP and IPF lung tissues revealed high-intensity staining in virtually all epithelial cells as well as alveolar macrophages and desquamated alveolar cells (Fig. 1*Ef*, 1*EH*). Thus consistent with the animal model, human pulmonary fibrosis exhibited marked induction of lung FIZZ2 expression in the same cell types.

### Regulation of FIZZ2 expression

Given that marked induction in AECs represented the major cellular source of FIZZ2 in BLM-induced lung fibrosis and human IPF, the regulation of this induction was analyzed in isolated AECs as well as in a human AEC line. Because the Th2 cytokines IL-4 and IL-13 are potent inducers of AEC FIZZ1 expression, and production of IL-17 and IFN- $\gamma$  is upregulated in the lung cells of BLM-treated mice (35, 36), these agents were analyzed for their ability to induce FIZZ2 in these cells using qPCR. The results revealed very low level expression in untreated rodent AECs, which was significantly upregulated by treatment with either IL-4 or IL-13 as early as 4 h of treatment, with a greater effect noted for IL-4 (Fig. 2*A*). FIZZ2 gene expression was significantly upregulated by IL-4 at 4-h and 8-h time points and by IL-13 at the 4-h time point ( $p < 0.05$ ). IFN- $\gamma$  and IL-17 did not induce FIZZ2 expression (Fig. 2*A*). Because human AEC is also a cellular source for FIZZ2 expression (23) and highly induced in IPF and NSIP lung tissues (Fig. 1*D*), regulation of its expression in human small airway epithelial cells was examined. Consistent with the rodent cells, human small airway epithelial cells also showed low-level FIZZ2 expression that was upregulated by treatment with either Th2 cytokine at the 8-h point ( $p = 0.042$  and  $p = 0.001$ , respectively), but not by IFN- $\gamma$  or IL-17 (Fig. 2*B*). Three doses of cytokines (2, 10, and 50 ng/ml for IFN- $\gamma$ ; 5, 10, and 50 ng/ml for IL-17) did not show effects on FIZZ2 expression in both rat AEC and human small airway epithelial cells (data not shown), even though the biological activity of the doses used above were confirmed by testing their known effects on the induction of MHC class I (37) and IL-6 (38), respectively (data not shown). In the case of the human cells, however, the fold-upregulation was not as great as in the rodent cells, and the effect of IL-13 was greater than that of IL-4. To put these findings in an in vivo context, the induction of FIZZ2 in the BLM model was analyzed in IL-4 and IL-4/IL-13



double KO mice. These Th2-deficient mice were previously shown to have significantly reduced pulmonary fibrosis associated with impaired induction of FIZZ1 expression (13). The results showed similar impairment of lung FIZZ2 induction as determined by qPCR in both Th2-deficient strains (Fig. 2C). Moreover, STAT6-deficient mice also showed similar impairment of lung FIZZ2 expression (Fig. 2D). The latter findings confirm the importance of Th2 cytokines in FIZZ2 induction in this model, as STAT6 signaling is known to mediate their effects (18). These results indicated that FIZZ2 expression in epithelial cells was driven by Th2-type cytokines via STAT6 signaling, suggesting a possible mechanism for its induction in pulmonary fibrosis.

### **FIZZ2 deficiency impaired BLM-induced pulmonary fibrosis**

A potentially important role for FIZZ2 in pathogenesis of fibrosis is suggested by its induction in both an animal model and human disease. This possibility was evaluated by comparing the extent of BLM-induced pulmonary fibrosis in FIZZ2 KO mice with that in their WT controls. As expected, WT mice exhibited significant fibrosis as manifested by an approximate doubling in lung hydroxyproline content along with elevations in extracellular matrix,  $\alpha$ -SMA, FIZZ1, telomerase reverse transcriptase (TERT), and cytokine expression (Fig. 3A–C). However, in FIZZ2 KO mice, these responses to BLM treatment were all significantly diminished with virtual complete suppression in certain parameters. Noteworthy was the virtually complete inhibition of BLM-induced expression of MCP-1 and FIZZ1, which are known to play significant roles in this animal model (Fig. 3C). Histological examination also confirmed that the BLM-induced lung injury in FIZZ2 KO mice was reduced compared with that in WT controls, showing only smaller scattered lesions with less cellularity. There was no significant morphology change observed between saline-treated WT and FIZZ2 KO mice (Fig. 3D). We next performed the total and differential BAL cell counting at day 4 after BLM/saline treatment by flow cytometry analysis. The results showed that BLM treatment caused significant increase in total BAL cell number in WT animals as expected. In FIZZ2 KO mice, BLM treatment also induced a similar fold-increase in total BAL cell number ( $p < 0.05$ ) although the absolute number of total BAL cells in KO mice was lower than that in WT mice. The differential cell counting revealed comparable BLM-induced fold-increases in numbers of neutrophils and CD3 T cells in WT and FIZZ2 KO mice, but the absolute cell numbers were lower in the FIZZ2 KO group. The absolute number of macrophages was also reduced in BLM-treated FIZZ2 KO mice (Fig. 3E). These results indicated that FIZZ2 deficiency reduced the absolute numbers of cells in BALF but did not significantly affect BLM-induced increase in BAL inflammatory cells.

Similarly, analysis of lung tissue CD3 T cell number by flow cytometry at day 4 post-BLM injection revealed similar BLM-induced increases in both WT and FIZZ2 KO mice ( $p < 0.05$  and  $p < 0.001$ , respectively). There was no clear difference observed between WT and FIZZ2 KO groups (Fig. 3F). Lung CD3 T cell number was also analyzed at day 14, and the data showed a similar pattern (data not shown). This suggested that FIZZ2 deficiency was also unimportant in BLM-induced T cell recruitment.

To assess further the potential effects of FIZZ2 deficiency on BLM-induced alterations in lung gene expression, cDNA microarray analysis was undertaken. Beyond confirmation of the gene expression studies described earlier, the results further showed significant suppression of at least 74 identifiable BLM-induced genes, including serum amyloid A3 (SAA3), which was not known to be associated with pulmonary fibrosis previously (Table II). The effects on a select set of extracellular matrix and protease genes were shown, which revealed uniformly consistent suppression in KO mice (Fig. 3G). The data discussed in this publication have been deposited in the National Center for Biotechnology Information Gene Expression Omnibus (GEO) database and are accessible through GEO series accession number GSE25640 (<http://www.ncbi.nlm.nih.gov/geo/query/acc.cgi?acc=GSE25640>). Another parameter of fibrosis is fibroblast proliferation, which was measured in primary cultures of murine lung fibroblasts in vitro. Whereas lung fibroblasts from WT BLM-treated mice exhibited increased proliferation relative to those obtained from saline-treated controls, this difference was essentially abolished in cells obtained from FIZZ2 KO mice (Fig. 3H).

Taken together, these findings suggested that FIZZ2 deficiency had profound and widespread effects on diverse parameters of pulmonary fibrosis, many of which are known to be important in pathogenesis of fibrosis.

### **FIZZ2 induced fibroblast activation and proliferation**

The dependence of BLM-induced pulmonary fibrosis on FIZZ2 indicated a role or roles for this molecule in mediating cellular processes essential for extracellular matrix deposition. To address this possibility, lung fibroblasts, as a key contributor to interstitial collagen deposition, were isolated and analyzed for their responses to FIZZ2 treatment in vitro. First, cDNA microarray analysis was undertaken to assess the spectrum of genes whose expression would be affected by this treatment. FIZZ2-treated MLFs exhibited significant (>2-fold) upregulation in 2174 and 989 genes at 2 and 6 h of treatment, respectively; whereas 896 genes and 491 genes were downregulated at 2- and 6-h points, respectively. Notably, groups of cytokine, chemokine, and a number of fibrosis-related extracellular matrix genes were affected by FIZZ2 treatment. Thus, type I procollagen gene was induced >3-fold by FIZZ2 as early as 2 h posttreatment and remained 1.5-fold elevated at 6 h. This stimulation of type I collagen expression was validated by qPCR and Western blotting analyses, which showed significant stimulation of expression at 6 h of treatment by 25 ng/ml FIZZ2 (Fig. 4A). To see if this effect could be synergized by treatment with TGF- $\beta$ , the cells were exposed to suboptimal doses of FIZZ2 (10 ng/ml) or TGF- $\beta$ 1 (0.1 ng/ml), or both. The results showed that whereas suboptimal doses of these molecules individually failed to affect type I procollagen mRNA levels in MLFs, the combination of both agents caused a synergistic stimulation (Fig. 4B). FIZZ2 effect on another parameter of fibroblast activation,  $\alpha$ -SMA expression or myofibroblast differentiation, was also evaluated by Western blotting. The results showed that MLF  $\alpha$ -SMA protein expression was also stimulated by FIZZ2 at doses as low as 25 ng/ml (Fig. 4C). Thus, the induction of lung FIZZ2 expression in pulmonary fibrosis might be a contributory mechanism for the fibroblast activation and myofibroblast differentiation that are believed to be essential for fibrogenesis.

Another key feature of fibrosis is fibroproliferation. There is evidence that FIZZ2 is a mitogenic factor for human pulmonary endothelial and smooth muscle cells (24). To determine whether FIZZ2 can stimulate fibroblast proliferation, MLFs were treated with various concentration of FIZZ2 and cell proliferation evaluated. The results showed that FIZZ2 significantly ( $p < 0.001$ ) stimulated fibroblast proliferation at doses as low as 10 ng/ml, which appears to be maximal because no further significant increase was noted at higher doses (Fig. 5A). Compared with the dose-response curve for stimulation of collagen expression (Fig. 4A), the FIZZ2 effect on proliferation was more potent. To explore a potential intracellular signaling mechanism involved in the proliferative effect of FIZZ2, its effects on activation of the known relevant signaling pathways were examined next. Phosphorylation status of the three key MAPKs (ERK, JNK, and p38) and AKT in FIZZ2-treated MLFs were analyzed by Western blotting. The results showed rapid (10 min) marked activation of ERK by FIZZ2, with lesser effects on AKT and p38 (Fig. 5B). JNK was not activated by FIZZ2 treatment. To see if the FIZZ2-induced activation of ERK was required for the effect on cell proliferation, the effect of pretreatment with the MEK/ERK inhibitor PD98059 was examined. This pretreatment with the inhibitor significantly suppressed FIZZ2-stimulated fibroblast proliferation compared with that in cells treated with FIZZ2 only ( $p < 0.05$ , Fig. 5C). Thus, FIZZ2 could promote fibroblast proliferation via signaling through ERK.

Finally, increased fibroblast and myofibroblast numbers could be due to, or enhanced by, suppression of (or enhanced resistance to) apoptosis. Fibroblasts were treated with TNF- $\alpha$  plus cycloheximide to induce apoptosis in the absence or presence of FIZZ2. Subsequent analysis by flow cytometry after annexin V-PI staining revealed that FIZZ2 did not significantly affect apoptosis in lung fibroblasts (data not shown). Thus, FIZZ2 might contribute to fibroproliferation primarily by enhancing cell proliferation and not by making fibroblasts more resistant to apoptosis.

### **FIZZ2 was essential for recruitment of BM cells into the lung**

Recruitment of cells from the BM to the lung is a notable feature of pulmonary fibrosis that has been shown to be essential for fibrogenesis in the BLM-induced mouse model (30, 39–41). Some of these cells express type I collagen and TERT in the rodent model and are important for the induction of lung TERT expression and the overall fibrotic response (30, 41). Because BLM-induced TERT expression is dependent on BM recruited cells (30, 41) and was inhibited in FIZZ2 KO mice (Fig. 3C), the role of FIZZ2 in BM cell recruitment was investigated. Moreover, another member of the FIZZ family, FIZZ1, is capable of recruiting macrophages and eosinophils (42). To first assess this possibility, whole rodent BM cells were analyzed for their ability to respond to FIZZ2 in a Boyden chamber assay. The results showed that these cells could migrate to increasing concentrations of FIZZ2 placed in the lower chamber, with rat cells having greater migration than the murine cells (Fig. 6A). This migratory activity was noted even after the BM cells were cultured in GM-CSF to promote differentiation to CD11c<sup>+</sup> dendritic cells (BMDCs) but significant only in BM cells from BLM-treated animals (Fig. 6B). To demonstrate the *in vivo* relevance of these *in vitro* findings, the effect of FIZZ2 deficiency on BM cell recruitment to the lung was evaluated in the BLM model using GFP-BM chimera mice. BM cells from GFP

transgenic mice were transplanted into WT or FIZZ2 KO mice to allow monitoring of BM cell recruitment by tracking the GFP marker. The results showed the presence of three distinct populations of adherent lung cells: one without GFP expression (gated as R1 in Fig. 6C), another with low-level GFP expression (R2), and a high GFP expressing one (R3). BLM treatment caused an increase in the high GFP<sup>+</sup> cells from 25 to 37.4%. However in FIZZ2 KO mice, the number of high GFP<sup>+</sup> cells was reduced at 10.1% (40% of WT), which was not significantly altered by BLM treatment at 10.4% (28% of WT). Based on forward light scatter, these high GFP expressing cells appeared to be larger than the low GFP expressing cells. Given the differential behavior of BMDCs from BLM-treated versus control mice (Fig. 6B), the identity of the high GFP<sup>+</sup> cells was examined to see if they express CD11c. Flow cytometry revealed that >85% of this cell fraction expressed CD11c (Table III). Transplantation of WT BM from GFP transgenic mice failed to alter the deficient pulmonary fibrosis in the FIZZ2 KO recipient mice (data not shown). Thus, the absence of FIZZ2 impaired BM cell recruitment and pulmonary fibrosis, which could not be corrected by transplantation of WT BM.

## Discussion

A myriad of inflammatory and fibrogenic cytokines such as TGF- $\beta$ , TNF- $\alpha$ , MCP-1, and a recently identified FIZZ/RELM family member FIZZ1 have been identified as important factors in the pathogenesis of pulmonary fibrosis (11, 43, 44), mediating the cross-talk between epithelial cells and adjacent fibroblasts, as well as induction of myofibroblast differentiation (11–13, 45). Despite this expanding list of genes important for fibrosis, the failure of therapeutic trials targeting some of these factors suggests that this list is probably incomplete. Moreover, with respect to the FIZZ family specifically, the actual identity of the human counterpart to rodent FIZZ1 remains uncertain, despite evidence that, at least functionally, human FIZZ2 may have similar properties as rodent FIZZ1. Previous studies in animal models indicate that FIZZ2 is a Th2 cytokine-inducible immunomodulatory molecule important in resisting gastrointestinal tract nematode infection, maintenance of colonic epithelium barrier function (22, 27), and promotion of airway inflammation and remodeling in an allergic airway disease model (18). However, its role in pulmonary fibrosis affecting the distal lung parenchyma, such as that associated with interstitial lung diseases, remains unknown. But recently there is increasing evidence of lung FIZZ2 expression being induced in human fibrotic lung diseases with significant tissue remodeling (23, 24). Moreover, human FIZZ2 is more homologous to rodent FIZZ2 than FIZZ1 (17) thus imparting greater human relevance to studies of rodent FIZZ2.

The potential importance of FIZZ2 was first suggested in this study by the induction of lung FIZZ2 expression in both the BLM-induced animal model and human patients with IPF and NSIP, in a manner that is similar to the high induction of its rodent family member, FIZZ1, in the same animal model (11). Consistent with previous studies, Th2 but not Th1 or Th17 cytokines were found to be effective in induction of FIZZ2 expression in both rodent AECs and human small airway epithelial cells. Moreover, studies using Th2-deficient as well as STAT6-deficient mice indicated their importance for FIZZ2 induction in the murine model of pulmonary fibrosis, thus affirming their importance *in vivo* as well. There is ample evidence to suggest that Th2-type cytokines, IL-4 and IL-13, are involved in fibrotic disease.

They are capable of stimulating myofibroblast differentiation and fibroblast proliferation (8, 43, 44, 46, 47). IL-4 and IL-13 are potent inducers of AEC FIZZ1 expression via STAT-6 (13). The demonstration that Th2 cytokines IL-4 and IL-13 could induce FIZZ2 expression in both animal AECs and human small airway epithelial cells argues for an important role for this molecule in pulmonary fibrosis.

To prove that it is essential for pulmonary fibrosis, the effect of FIZZ2 deficiency on BLM-induced pulmonary fibrosis was evaluated. The findings using FIZZ2 KO mice revealed impaired fibrosis in the absence of FIZZ2 that was accompanied by reduction in BLM-induced expression of cytokines, extracellular matrix, FIZZ1, TERT, and  $\alpha$ -SMA. However, FIZZ2 deficiency failed to impact significantly BLM-induced increases in cells in the BAL or T cells in lung tissue. Given this multitude of effects, the role of FIZZ2 in this model of fibrosis is likely to lie upstream of these known key processes critical to the fibrogenic response. Additionally, however, it could have direct regulatory effects on fibroblast proliferation, apoptosis, activation, and myofibroblast differentiation, which are known to be important in fibrogenesis. Increased numbers of fibroblasts is a characteristic feature of pulmonary fibrosis, and augmented fibroblast proliferation may contribute to the progressive fibrosis. FIZZ2 has proliferative effects on intestinal and lung cells (15, 23). Moreover, its expression is greatest in proliferative epithelia at the bases of crypts in colon and markedly increased in tumors in *min* mice, consistent with a role in cell proliferation (15). The current study revealed that FIZZ2 had a proliferative effect on primary cultured lung fibroblasts, unlike FIZZ1 (14). Similar activity in human A549 cells and lung vascular smooth muscle cells has been observed in response to FIZZ2 treatment (23). Cell proliferation, differentiation, survival, and apoptosis are known to be regulated by certain MAPK pathways (48, 49). The PI3K–AKT signaling pathway is more associated with cell survival (50). In the case of FIZZ2-mediated fibroblast proliferation, ERK1/2 activation was associated with this effect, and treatment with the ERK inhibitor PD98059 abrogated the proliferative effect. However, in contrast to FIZZ1 (14), FIZZ2 did not provide significant protection against apoptosis, suggesting somewhat different activities between these two members of the FIZZ family. FIZZ2 stimulation of vascular smooth muscle cell proliferation in response to hypoxia is found to have similar dependence on MAPK signaling (23).

Given the key role of myofibroblast, which functions as a major source of extracellular matrix and as an inflammatory cell (45), the ability of FIZZ2 to activate fibroblasts and regulate myofibroblast differentiation was examined. In addition to enhancing cell proliferation, FIZZ2 was able to activate directly lung fibroblasts by stimulating extracellular matrix expression. This activation was accompanied by enhancement of  $\alpha$ -SMA expression, indicative of myofibroblast differentiation. Thus, FIZZ2 has the capability of directly affecting fibroblast function in a manner that is conducive to the induction and/or propagation of fibrosis. Certainly, its importance in fibrosis is already revealed by the studies using FIZZ2 KO mice.

The importance of recruited BM-derived cells is suggested by studies in both animal models and human pulmonary fibrosis (30, 39–41). The lack of TERT induction in FIZZ2 KO mice suggested the possibility that BM cell recruitment may be impaired as this is shown to be dependent on influx of BM-derived cells (41). The ability of FIZZ2 to promote cell

migration is not unprecedented, as peritoneal injection of FIZZ1 recruits eosinophils and lymphocytes, and FIZZ1 is capable of inducing eosinophil chemotaxis (42). The ability of FIZZ2 to recruit directly BM-derived cells was evaluated using the Boyden chamber assay. The results indicated that FIZZ2 was effective in promoting BM cell migration, and notably BM-derived CD11c<sup>+</sup> DCs. To put this in an in vivo context, GFP-BM chimera mice were analyzed for recruitment of GFP<sup>+</sup> (i.e., BM derived) cells into lung tissue in recipient mice sufficient (WT) or deficient (FIZZ2 KO) in FIZZ2 expression. Transplantation of WT BM cells from GFP transgenic mice to FIZZ2 KO recipients resulted in reduced numbers of BM-derived cells in both control and BLM-treated animals relative to that in WT recipients. Moreover, BLM treatment failed to induce an increase in the number of lung BM-derived cells in FIZZ2-deficient mice. Notably, transplantation of WT BM cells was insufficient to correct the impaired fibrosis in FIZZ2 KO mice, consistent with the hypothesis that the recruited BM cells play an important role in fibrosis. It is also noteworthy that the predominant recruited BM cell type expressed CD11c, a marker of DCs. A recent study of murine hepatic fibrosis revealed a 5-fold expansion in hepatic DCs capable of activating hepatic stellate cells, NK cells, and T cells to mediate inflammation, cell proliferation, and production of potent immune responses (51). Our findings strongly suggested that FIZZ2 promoted the pulmonary fibrotic process, at least in part, through recruitment of BM-derived cells. There is evidence for a role of DCs in pulmonary fibrosis (52), and their presence in human interstitial lung disease including IPF have been documented (53, 54).

The mechanism of BM cell recruitment by FIZZ2 may also be indirect via the SDF-1/CXCR4 axis. This axis is shown to play a role in recruiting BM cells to the lung in the BLM and hypoxia-induced animal models (30, 55, 56). The SDF-1 levels in serum and BALF were increased and accompanied by increased number of CXCR4<sup>+</sup> cells in the lung but with a decreased number in the BM. In addition, neutralizing Ab against SDF-1, or antagonists of CXCR4, attenuate pulmonary fibrosis (30, 55, 57, 58). Furthermore, an ex vivo lung organ culture study suggests that SDF-1/CXCR4 may be involved in the recruitment of circulating cells into the lung by FIZZ1 in hypoxia as demonstrated by its ability to induce SDF-1 expression in lung organ slices (59). Thus, it is possible that FIZZ2 might function in a similar manner by regulation of SDF-1 production in BLM-induced pulmonary fibrosis.

Taken together, the findings in the current study indicated that FIZZ2 was a Th2-regulated factor with potential profibrogenic activity. It was shown to be essential for pulmonary fibrosis in an animal model. Because the expression pattern of FIZZ2 in this animal model was similar to that in human pulmonary fibrosis (IPF, NSIP), and FIZZ2 induction in both animal and human epithelial cells was regulated by Th2 cytokines, the importance of FIZZ2 function in the animal model might be relevant to human fibrotic pulmonary diseases. Further studies of human FIZZ2 in these diseases are warranted.

## Acknowledgments

We are grateful to Nicholas Lukacs for provision of STAT6 KO mice and Andrew McKenzie for provision of the IL-4 and IL-4/IL-13 KO mice.

This work was supported by the Korea Research Foundation funded by the Korean Government (Ministry of Education and Human Resources Development Grant KRF-2007-531-E00011 to M.J.C.), by the National Institutes of Health (Grants HL028737, HL031936, HL052285, HL077297, and HL091775 to S.H.P.), and by Grant

DK020572 from the National Institute of Diabetes and Digestive and Kidney Diseases to the Affymetrix Microarray Core of the Michigan Diabetes Research and Training Center.

## Abbreviations used in this article

<b>AEC</b>	alveolar epithelial cell
<b>BAL</b>	bronchoalveolar lavage
<b>BALF</b>	bronchoalveolar lavage fluid
<b>BLM</b>	bleomycin
<b>BM</b>	bone marrow
<b>BMDC</b>	bone marrow-derived dendritic cell
<b>FIZZ</b>	found in inflammatory zone
<b>GEO</b>	Gene Expression Omnibus
<b>IPF</b>	idiopathic pulmonary fibrosis
<b>KO</b>	knockout
<b>MLF</b>	mouse lung fibroblast
<b>MTS</b>	3-(4,5-dimethylthiazol-2-yl)-5-(3-carboxymethoxyphenyl)- 2-(4-sulfophenyl)-2H-tetrazolium
<b>NSIP</b>	nonspecific interstitial pneumonia
<b>PI</b>	propidium iodide
<b>qPCR</b>	quantitative PCR
<b>RELM</b>	resistin-like molecule
<b><math>\alpha</math>-SMA</b>	$\alpha$ -smooth muscle actin
<b>TERT</b>	telomerase reverse transcriptase
<b>WT</b>	wild-type

## References

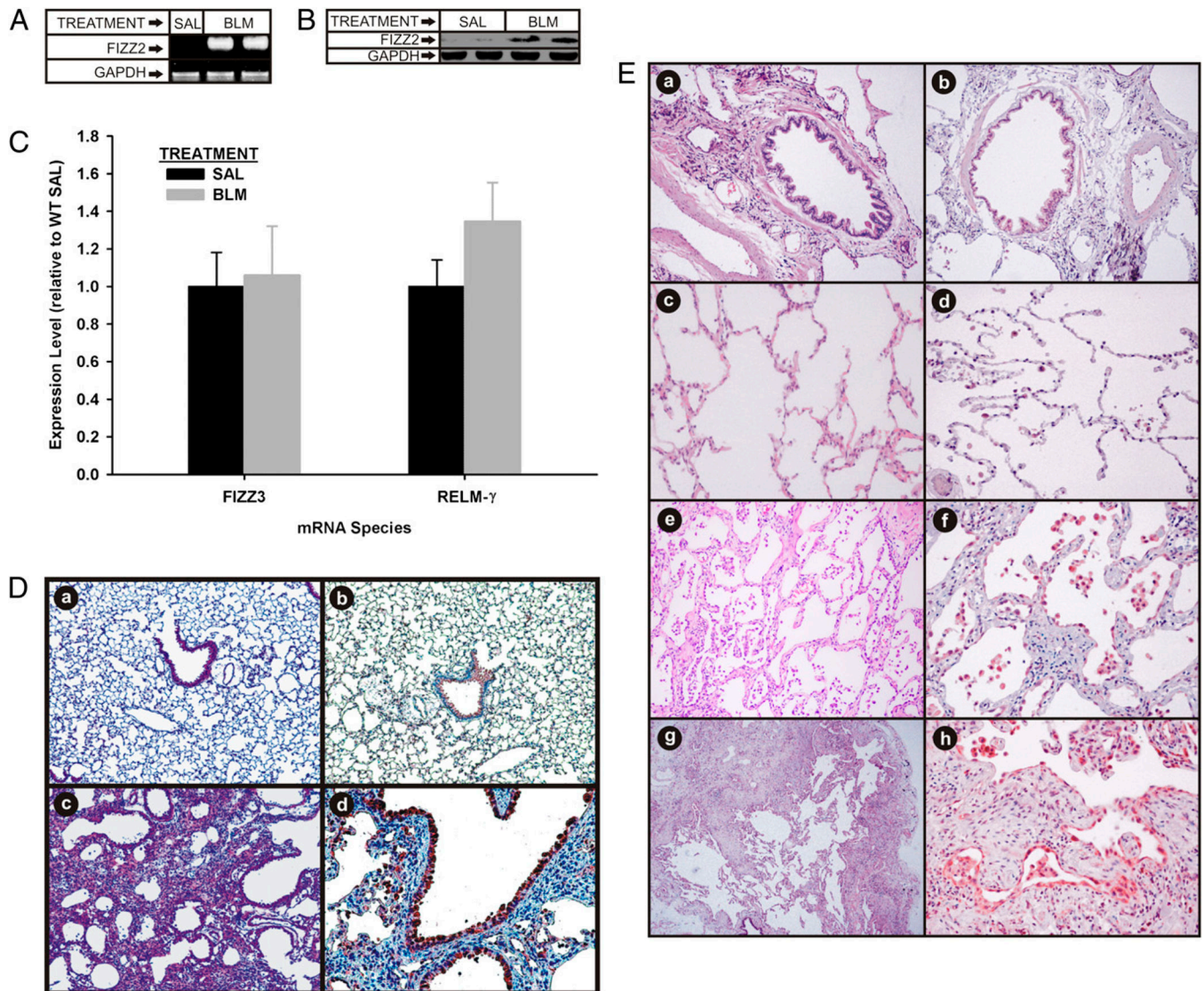
1. Gross TJ, Hunninghake GW. Idiopathic pulmonary fibrosis. *N. Engl. J. Med.* 2001; 345:517–525. [PubMed: 11519507]
2. Mason RJ, Schwarz MI, Hunninghake GW, Musson RA. NHLBI Workshop Summary. Pharmacological therapy for idiopathic pulmonary fibrosis. Past, present, and future. *Am. J. Respir. Crit. Care Med.* 1999; 160:1771–1777. [PubMed: 10556155]
3. Elias JA, Zhu Z, Chupp G, Homer RJ. Airway remodeling in asthma. *J. Clin. Invest.* 1999; 104:1001–1006. [PubMed: 10525034]
4. Roche WR, Beasley R, Williams JH, Holgate ST. Subepithelial fibrosis in the bronchi of asthmatics. *Lancet.* 1989; 1:520–524. [PubMed: 2466184]
5. Evans JN, Kelley J, Low RB, Adle KB. Increased contractility of isolated lung parenchyma in an animal model of pulmonary fibrosis induced by bleomycin. *Am. Rev. Respir. Dis.* 1982; 125:89–94. [PubMed: 6175262]
6. Phan SH, Varani J, Smith D. Rat lung fibroblast collagen metabolism in bleomycin-induced pulmonary fibrosis. *J. Clin. Invest.* 1985; 76:241–247. [PubMed: 2410457]

7. Zhang HY, Gharaee-Kermani M, Zhang K, Karmioli S, Phan SH. Lung fibroblast alpha-smooth muscle actin expression and contractile phenotype in bleomycin-induced pulmonary fibrosis. *Am. J. Pathol.* 1996; 148:527–537. [PubMed: 8579115]
8. Jakubzick C, Choi ES, Joshi BH, Keane MP, Kunkel SL, Puri RK, Hogaboam CM. Therapeutic attenuation of pulmonary fibrosis via targeting of IL-4- and IL-13-responsive cells. *J. Immunol.* 2003; 171:2684–2693. [PubMed: 12928422]
9. Selman M, King TE, Pardo A. American Thoracic Society; European Respiratory Society; American College of Chest Physicians. Idiopathic pulmonary fibrosis: prevailing and evolving hypotheses about its pathogenesis and implications for therapy. *Ann. Intern. Med.* 2001; 134:136–151. [PubMed: 11177318]
10. Zhang K, Rekhter MD, Gordon D, Phan SH. Myofibroblasts and their role in lung collagen gene expression during pulmonary fibrosis. A combined immunohistochemical and in situ hybridization study. *Am. J. Pathol.* 1994; 145:114–125. [PubMed: 7518191]
11. Liu T, Dhanasekaran SM, Jin H, Hu B, Tomlins SA, Chinnaiyan AM, Phan SH. FIZZ1 stimulation of myofibroblast differentiation. *Am. J. Pathol.* 2004; 164:1315–1326. [PubMed: 15039219]
12. Liu T, Hu B, Choi YY, Chung M, Ullenbruch M, Yu H, Lowe JB, Phan SH. Notch1 signaling in FIZZ1 induction of myofibroblast differentiation. *Am. J. Pathol.* 2009; 174:1745–1755. [PubMed: 19349363]
13. Liu T, Jin H, Ullenbruch M, Hu B, Hashimoto N, Moore B, McKenzie A, Lukacs NW, Phan SH. Regulation of found in inflammatory zone 1 expression in bleomycin-induced lung fibrosis: role of IL-4/IL-13 and mediation via STAT-6. *J. Immunol.* 2004; 173:3425–3431. [PubMed: 15322207]
14. Chung MJ, Liu T, Ullenbruch M, Phan SH. Antiapoptotic effect of found in inflammatory zone (FIZZ)1 on mouse lung fibroblasts. *J. Pathol.* 2007; 212:180–187. [PubMed: 17492827]
15. Stepan CM, Brown EJ, Wright CM, Bhat S, Banerjee RR, Dai CY, Enders GH, Silberg DG, Wen X, Wu D, Lazar MA. A family of tissue-specific resistin-like molecules. *Proc. Natl. Acad. Sci. USA.* 2001; 98:502–506. [PubMed: 11209052]
16. Gerstmayer B, Küsters D, Gebel S, Müller T, Van Miert E, Hofmann K, Bosio A. Identification of RELMgamma, a novel resistin-like molecule with a distinct expression pattern. *Genomics.* 2003; 81:588–595. [PubMed: 12782128]
17. Holcomb IN, Kabakoff RC, Chan B, Baker TW, Gurney A, Henzel W, Nelson C, Lowman HB, Wright BD, Skelton NJ, et al. FIZZ1, a novel cysteine-rich secreted protein associated with pulmonary inflammation, defines a new gene family. *EMBO J.* 2000; 19:4046–4055. [PubMed: 10921885]
18. Mishra A, Wang M, Schlotman J, Nikolaidis NM, DeBrosse CW, Karow ML, Rothenberg ME. Resistin-like molecule-beta is an allergen-induced cytokine with inflammatory and remodeling activity in the murine lung. *Am. J. Physiol. Lung Cell. Mol. Physiol.* 2007; 293:L305–L313. [PubMed: 17545488]
19. Shojima N, Ogihara T, Inukai K, Fujishiro M, Sakoda H, Kushiyaama A, Katagiri H, Anai M, Ono H, Fukushima Y, et al. Serum concentrations of resistin-like molecules beta and gamma are elevated in high-fat-fed and obese db/db mice, with increased production in the intestinal tract and bone marrow. *Diabetologia.* 2005; 48:984–992. [PubMed: 15834545]
20. Kushiyaama A, Shojima N, Ogihara T, Inukai K, Sakoda H, Fujishiro M, Fukushima Y, Anai M, Ono H, Horike N, et al. Resistin-like molecule beta activates MAPKs, suppresses insulin signaling in hepatocytes, and induces diabetes, hyperlipidemia, and fatty liver in transgenic mice on a high fat diet. *J. Biol. Chem.* 2005; 280:42016–42025. [PubMed: 16243841]
21. Artis D, Wang ML, Keilbaugh SA, He W, Brenes M, Swain GP, Knight PA, Donaldson DD, Lazar MA, Miller HR, et al. RELMbeta/FIZZ2 is a goblet cell-specific immune-effector molecule in the gastrointestinal tract. *Proc. Natl. Acad. Sci. USA.* 2004; 101:13596–13600. [PubMed: 15340149]
22. Hogan PS, Seidu L, Blanchard C, Groschwitz K, Mishra A, Karow ML, Ahrens R, Artis D, Murphy AJ, Valenzuela DM, et al. Resistin-like molecule beta regulates innate colonic function: barrier integrity and inflammation susceptibility. *J. Allergy Clin. Immunol.* 2006; 118:257–268. [PubMed: 16815164]

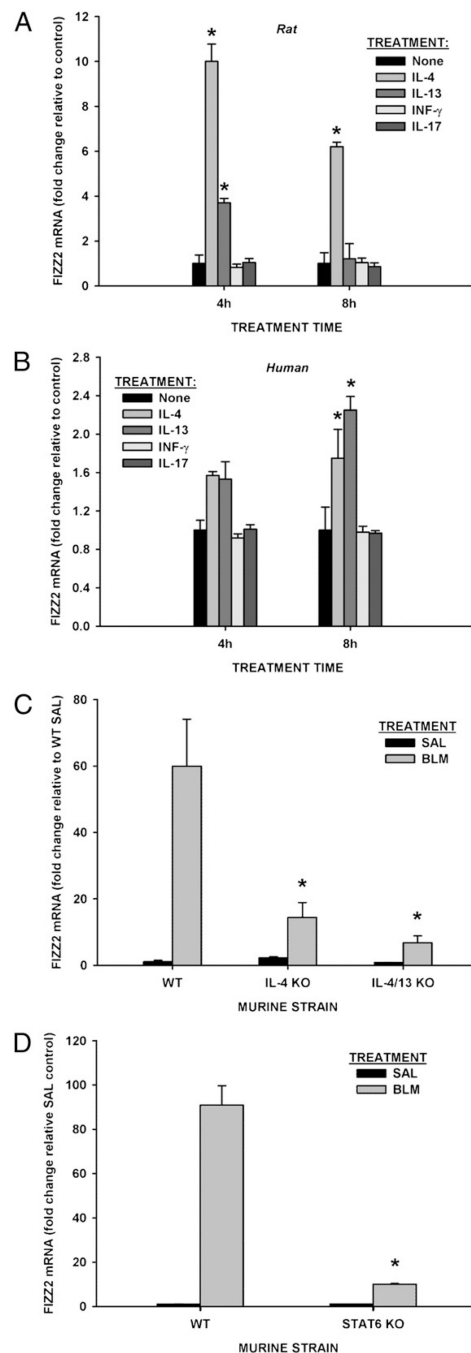


23. Renigunta A, Hild C, Rose F, Klepetko W, Grimminger F, Seeger W, Hänze J. Human RELMbeta is a mitogenic factor in lung cells and induced in hypoxia. *FEBS Lett.* 2006; 580:900–903. [PubMed: 16427636]
24. Angelini DJ, Su Q, Yamaji-Kegan K, Fan C, Teng X, Hassoun PM, Yang SC, Champion HC, Tudor RM, Johns RA. Resistin-like molecule-beta in scleroderma-associated pulmonary hypertension. *Am. J. Respir. Cell Mol. Biol.* 2009; 41:553–561. [PubMed: 19251945]
25. Homer JR. Airway remodeling and RELM-beta. *Am. J. Physiol. Lung Cell. Mol. Physiol.* 2007; 293:L303–L304. [PubMed: 17586697]
26. Brasch-Andersen C, Haagerup A, Børghlum AD, Vestbo J, Kruse TA. Highly significant linkage to chromosome 3q13.31 for rhinitis and related allergic diseases. *J. Med. Genet.* 2006; 43:e10. [PubMed: 16525028]
27. McVay LD, Keilbaugh SA, Wong TM, Kierstein S, Shin ME, Lehrke M, Lefterova MI, Shifflett DE, Barnes SL, Cominelli F, et al. Absence of bacterially induced RELMbeta reduces injury in the dextran sodium sulfate model of colitis. *J. Clin. Invest.* 2006; 116:2914–2923. [PubMed: 17024245]
28. McKenzie GJ, Fallon PG, Emson CL, Grecis RK, McKenzie AN. Simultaneous disruption of interleukin (IL)-4 and IL-13 defines individual roles in T helper cell type 2-mediated responses. *J. Exp. Med.* 1999; 189:1565–1572. [PubMed: 10330435]
29. Kaplan MH, Schindler U, Smiley ST, Grusby MJ. Stat6 is required for mediating responses to IL-4 and for development of Th2 cells. *Immunity.* 1996; 4:313–319. [PubMed: 8624821]
30. Hashimoto N, Jin H, Liu T, Chensue W, Phan SH. Bone marrow-derived progenitor cells in pulmonary fibrosis. *J. Clin. Invest.* 2004; 113:243–252. [PubMed: 14722616]
31. Dobbs LG. Isolation and culture of alveolar type II cells. *Am. J. Physiol.* 1990; 258:L134–L147. [PubMed: 2185652]
32. Edwards CA, O'Brien WD Jr. Modified assay for determination of hydroxyproline in a tissue hydrolyzate. *Clin. Chim. Acta.* 1980; 104:161–167. [PubMed: 7389130]
33. Irizarry RA, Hobbs B, Collin F, Beazer-Barclay YD, Antonellis KJ, Scherf U, Speed TP. Exploration, normalization, and summaries of high density oligonucleotide array probe level data. *Biostatistics.* 2003; 4:249–264. [PubMed: 12925520]
34. Ritchie ME, Diyagama D, Neilson J, van Laar R, Dobrovic A, Holloway A, Smyth GK. Empirical array quality weights in the analysis of microarray data. *BMC Bioinformatics.* 2006; 7:261. [PubMed: 16712727]
35. Wilson MS, Madala SK, Ramalingam TR, Gochuico BR, Rosas IO, Cheever AW, Wynn TA. Bleomycin and IL-1beta-mediated pulmonary fibrosis is IL-17A dependent. *J. Exp. Med.* 2010; 207:535–552. [PubMed: 20176803]
36. Segel MJ, Izbicki G, Cohen PY, Or R, Christensen TG, Wallach-Dayana SB, Breuer R. Role of interferon-gamma in the evolution of murine bleomycin lung fibrosis. *Am. J. Physiol. Lung Cell. Mol. Physiol.* 2003; 285:L1255–L1262. [PubMed: 12857673]
37. Gao J, De P, Banerjee AK. Human parainfluenza virus type 3 up-regulates major histocompatibility complex class I and II expression on respiratory epithelial cells: involvement of a STAT1- and CIITA-independent pathway. *J. Virol.* 1999; 73:1411–1418. [PubMed: 9882346]
38. Hwang SY, Kim JY, Kim KY, Park MK, Moon Y, Kim UW, Kim HY. IL-17 induces production of IL-6 and IL-8 in rheumatoid arthritis synovial fibroblasts via NF-kappaB- and PI3-kinase/Akt-dependent pathways. *Arthritis Res. Ther.* 2004; 6:R120–R128. [PubMed: 15059275]
39. Strieter RM, Keeley EC, Hughes MA, Burdick MD, Mehrad B. The role of circulating mesenchymal progenitor cells (fibrocytes) in the pathogenesis of pulmonary fibrosis. *J. Leukoc. Biol.* 2009; 86:1111–1118. [PubMed: 19581373]
40. Moeller AS, Gilpin SE, Ask K, Cox G, Cook D, Gaudie J, Margetts PJ, Farkas L, Dobranowski J, Boylan C, et al. Circulating fibrocytes are an indicator of poor prognosis in idiopathic pulmonary fibrosis. *Am. J. Respir. Crit. Care Med.* 2009; 179:588–594. [PubMed: 19151190]
41. Liu T, Chung MJ, Ullenbruch M, Yu H, Jin H, Hu B, Choi YY, Ishikawa F, Phan SH. Telomerase activity is required for bleomycin-induced pulmonary fibrosis in mice. *J. Clin. Invest.* 2007; 117:3800–3809. [PubMed: 18008008]

42. Munitz A, Waddell A, Seidu L, Cole ET, Ahrens R, Hogan SP, Rothenberg ME. Resistin-like molecule alpha enhances myeloid cell activation and promotes colitis. *J. Allergy Clin. Immunol.* 2008; 122:1200.e1–1207.e1. [PubMed: 19084112]
43. Gharaee-Kermani M, Gyetko MR, Hu B, Phan SH. New insights into the pathogenesis and treatment of idiopathic pulmonary fibrosis: a potential role for stem cells in the lung parenchyma and implications for therapy. *Pharm. Res.* 2007; 24:819–841. [PubMed: 17333393]
44. Gharaee-Kermani M, Phan SH. Role of cytokines and cytokine therapy in wound healing and fibrotic diseases. *Curr. Pharm. Des.* 2001; 7:1083–1103. [PubMed: 11472255]
45. Phan SH. The myofibroblast in pulmonary fibrosis. *Chest.* 2002; 122(6, Suppl):286S–289S. [PubMed: 12475801]
46. Matthey DL, Dawes PT, Nixon NB, Slater H. Transforming growth factor beta 1 and interleukin 4 induced alpha smooth muscle actin expression and myofibroblast-like differentiation in human synovial fibroblasts in vitro: modulation by basic fibroblast growth factor. *Ann. Rheum. Dis.* 1997; 56:426–431. [PubMed: 9486005]
47. Jakubzick C, Choi ES, Kunkel SL, Joshi BH, Puri RK, Hogaboam CM. Impact of interleukin-13 responsiveness on the synthetic and proliferative properties of Th1- and Th2-type pulmonary granuloma fibroblasts. *Am. J. Pathol.* 2003; 162:1475–1486. [PubMed: 12707030]
48. Xia Z, Dickens M, Raingeaud J, Davis RJ, Greenberg ME. Opposing effects of ERK and JNK-p38 MAP kinases on apoptosis. *Science (New York, N.Y.)*. 1995; 270:1326–1331.
49. Sebolt-Leopold JS, Herrera R. Targeting the mitogen-activated protein kinase cascade to treat cancer. *Nat. Rev. Cancer.* 2004; 4:937–947. [PubMed: 15573115]
50. Roymans D, Slegers H. Phosphatidylinositol 3-kinases in tumor progression. *Eur. J. Biochem.* 2001; 268:487–498. [PubMed: 11168386]
51. Connolly MK, Bedrosian AS, Mallen-St Clair J, Mitchell AP, Ibrahim J, Stroud A, Pachter HL, Bar-Sagi D, Frey AB, Miller G. In liver fibrosis, dendritic cells govern hepatic inflammation in mice via TNF-alpha. *J. Clin. Invest.* 2009; 119:3213–3225. [PubMed: 19855130]
52. Bantsimba-Malanda C, Marchal-Sommé J, Goven D, Freynet O, Michel L, Crestani B, Soler P. A role for dendritic cells in bleomycin-induced pulmonary fibrosis in mice? *Am. J. Respir. Crit. Care Med.* 2010; 182:385–395. [PubMed: 20395561]
53. Marchal-Sommé J, Uzunhan Y, Marchand-Adam S, Kambouchner M, Valeyre D, Crestani B, Soler P. Dendritic cells accumulate in human fibrotic interstitial lung disease. *Am. J. Respir. Crit. Care Med.* 2007; 176:1007–1014. [PubMed: 17717200]
54. Tsoumakidou M, Karagiannis KP, Bouloukaki I, Zakyntinos S, Tzanakis N, Siafakas NM. Increased bronchoalveolar lavage fluid CD1c expressing dendritic cells in idiopathic pulmonary fibrosis. *Respiration.* 2009; 78:446–452. [PubMed: 19556741]
55. Phillips RJ, Burdick MD, Hong K, Lutz MA, Murray LA, Xue YY, Belperio JA, Keane MP, Strieter RM. Circulating fibrocytes traffic to the lungs in response to CXCL12 and mediate fibrosis. *J. Clin. Invest.* 2004; 114:438–446. [PubMed: 15286810]
56. Ceradini DJ, Kulkarni AR, Callaghan MJ, Tepper OM, Bastidas N, Kleinman ME, Capla JM, Galiano RD, Levine JP, Gurtner GC. Progenitor cell trafficking is regulated by hypoxic gradients through HIF-1 induction of SDF-1. *Nat. Med.* 2004; 10:858–864. [PubMed: 15235597]
57. Xu J, Mora A, Shim H, Stecenko A, Brigham KL, Rojas M. Role of the SDF-1/CXCR4 axis in the pathogenesis of lung injury and fibrosis. *Am. J. Respir. Cell Mol. Biol.* 2007; 37:291–299. [PubMed: 17463394]
58. Song JS, Kang CM, Kang HH, Yoon HK, Kim YK, Kim KH, Moon HS, Park SH. Inhibitory effect of CXC chemokine receptor-4 antagonist AMD3100 on bleomycin induced murine pulmonary fibrosis. *Exp. Mol. Med.* 2010; 42:465–472. [PubMed: 20498529]
59. Yamaji-Kegan K, Su Q, Angelini DJ, Champion HC, Johns RA. Hypoxia-induced mitogenic factor has proangiogenic and proinflammatory effects in the lung via VEGF and VEGF receptor-2. *Am. J. Physiol. Lung Cell. Mol. Physiol.* 2006; 291:L1159–L1168. [PubMed: 16891392]

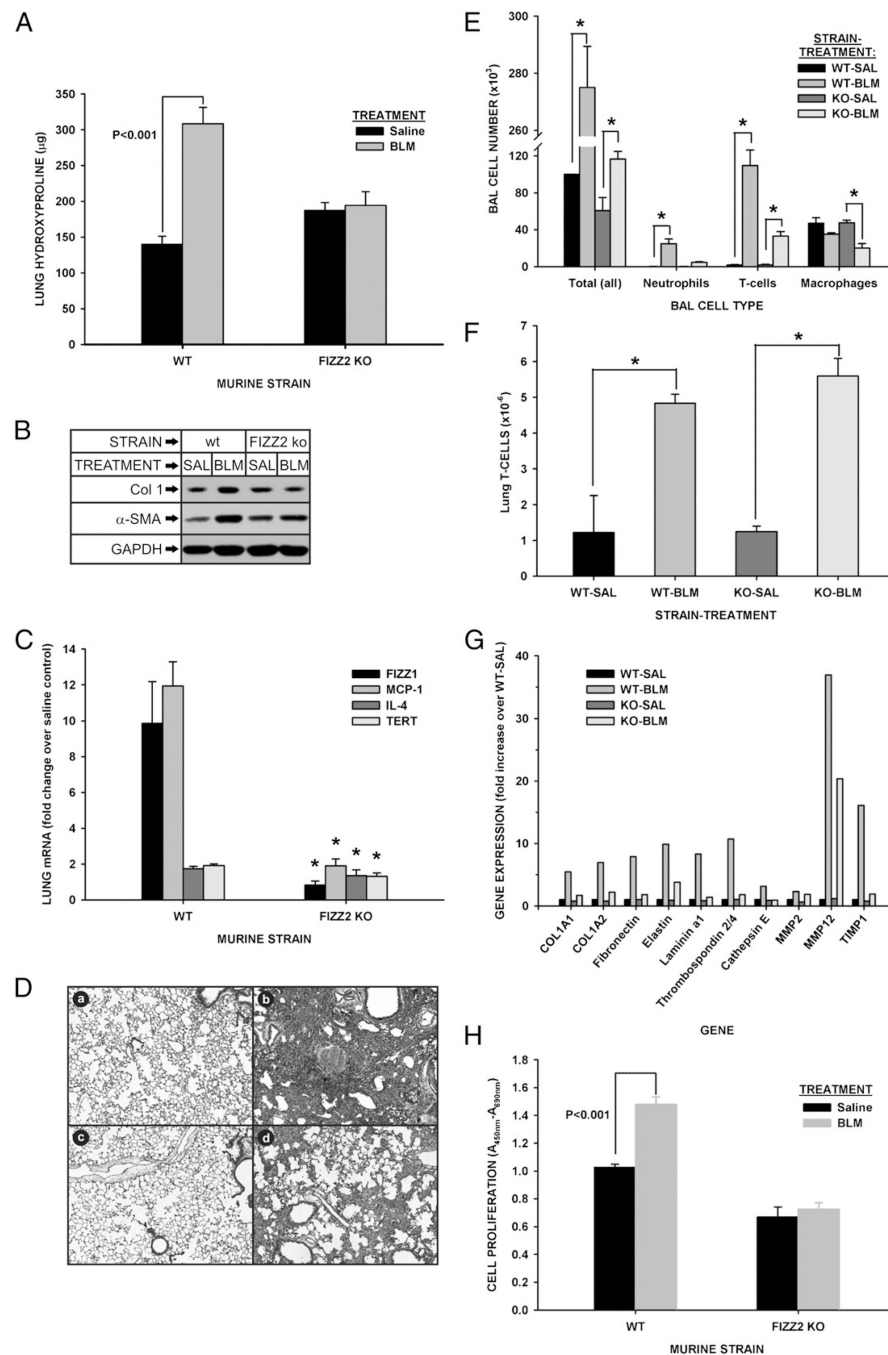


**FIGURE 1.** FIZZ2, FIZZ3, and RELM- $\gamma$  expression in pulmonary fibrosis. *A* and *B*, Murine lungs from saline (SAL)- or BLM-treated mice were analyzed for FIZZ2 mRNA (*A*) and protein (*B*) by RT-PCR and Western blotting, respectively. GAPDH protein served as a loading control. *C*, FIZZ3 and RELM- $\gamma$  mRNA levels in SAL- or BLM-treated mouse lungs. *D*, Representative lung tissue section from day 14 BLM (*c, d*) or saline-treated (*a, b*) mice were stained with H&E (*a, c*) or immunostained for FIZZ2 protein (*b, d*). Original magnification  $\times 40$  (*a, b*) and  $\times 100$  (*c, d*). *E*, Human lung tissues from normal controls (*a-d*) or patients with NSIP (*e, f*) or IPF (*g, h*) were stained with H&E (*a, c, e, g*) or immunostained for FIZZ2 protein (*b, d, f, h*). In both *D* and *E*, control staining using nonimmune IgG was negative. Original magnification  $\times 100$  (*c-e, g*);  $\times 200$  (*a, b, f, h*).

**FIGURE 2.**

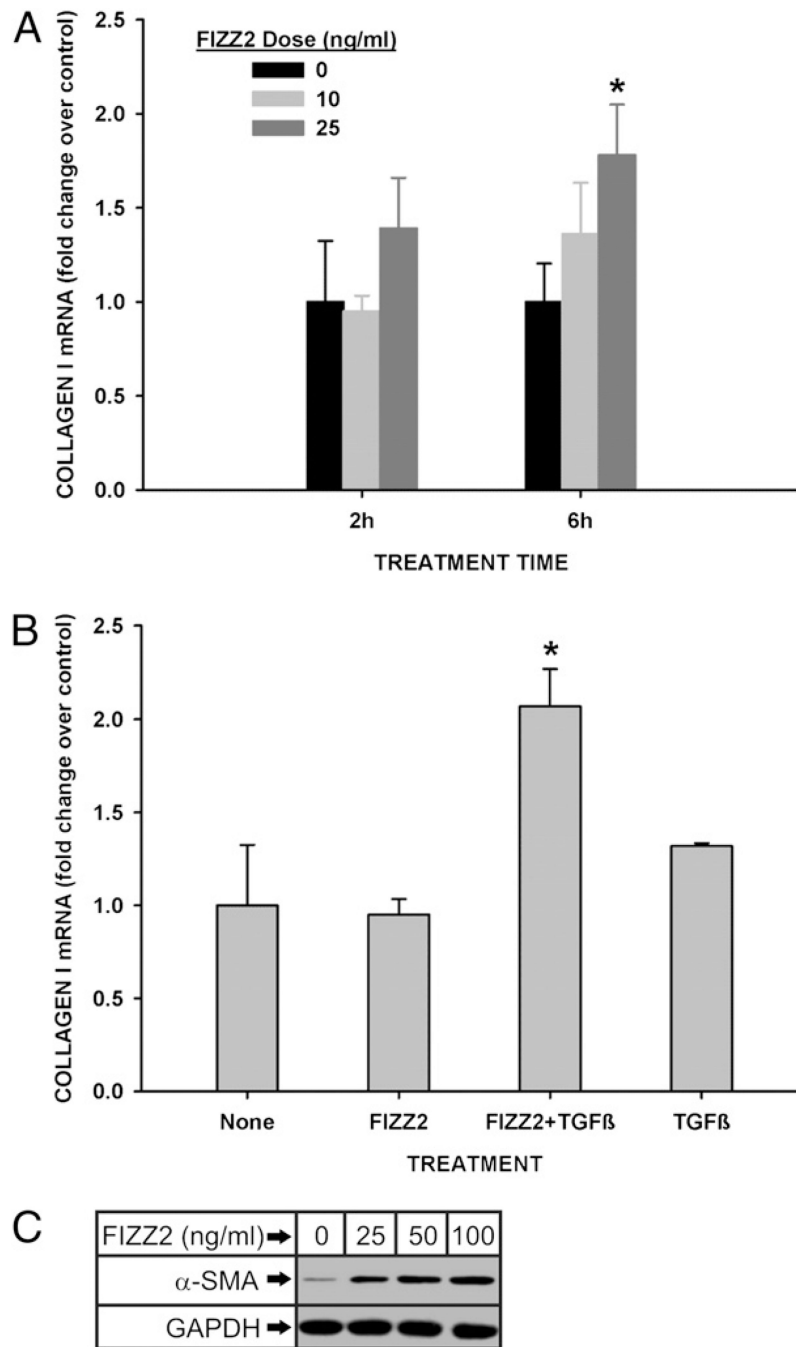
Cytokine regulation of FIZZ2 expression in AECs. *A* and *B*, Rat AECs (*A*) or human small airway epithelial cells (*B*) were treated with IL-4, IL-13, IFN- $\gamma$ , or IL-17 as indicated. At the end of incubation, total cell RNA was harvested for FIZZ2 mRNA analysis by qPCR. *C* and *D*, Lungs from the indicated strains of mice treated with saline (SAL) or BLM (on day 7) were similarly analyzed for FIZZ2 mRNA. The amount of FIZZ2 mRNA analyzed by qPCR was normalized to the GAPDH control signal and expressed as fold change over untreated or SAL-treated controls ( $2^{-CT}$ ). Results are shown as mean  $\pm$  SE of triplicate

samples.  $*p < 0.05$  compared with respective control (“None” in A and B, or WT SAL-treated controls in C and D) mean values.

**FIGURE 3.**

Effect of FIZZ2 deficiency on BLM-induced pulmonary fibrosis. **A**, WT control or FIZZ2 KO mice were treated with saline (SAL) or BLM as indicated, and 21 d later the lungs were harvested and analyzed for lung hydroxyproline content. The values are expressed as percentages of their respective SAL controls. Data are shown as mean  $\pm$  SE with five mice in each group. **B**, Type I collagen and  $\alpha$ -SMA protein in these lungs were also analyzed by Western blotting. A representative blot from four to five mice in each group is shown. **C**, For lung mRNA analysis by qPCR, the lungs were harvested on day 7 after SAL or BLM

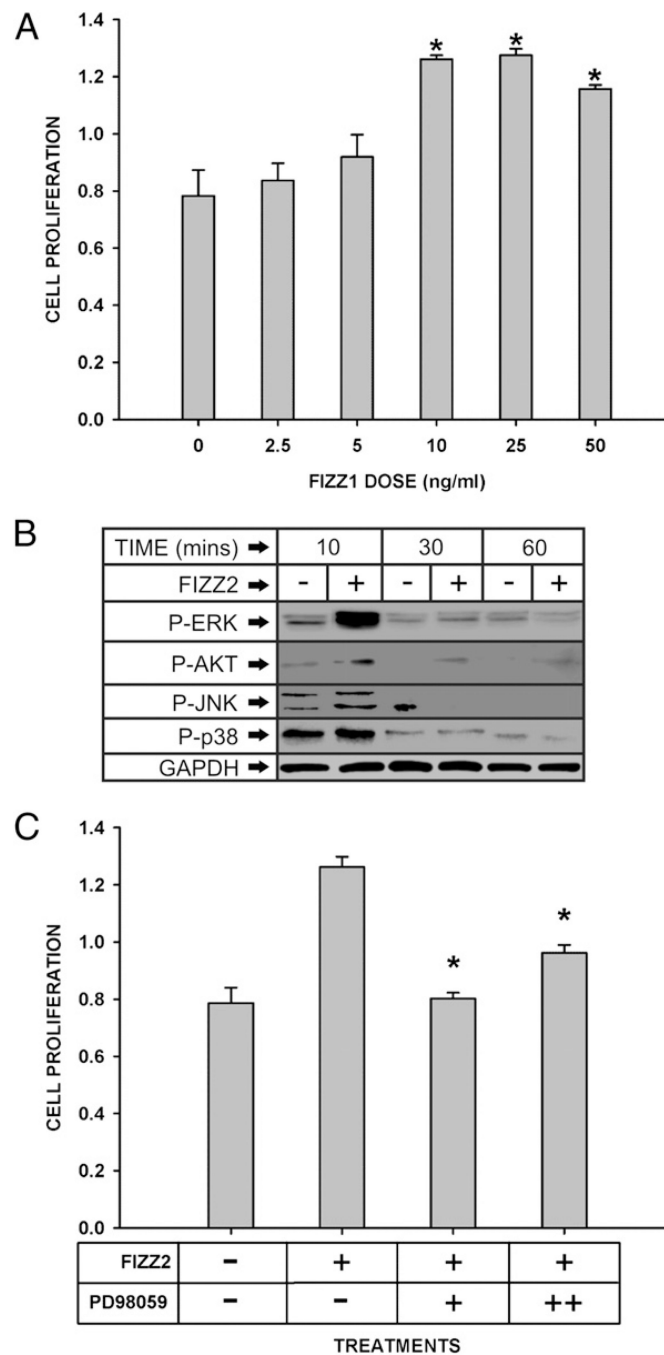
treatment. Results are expressed as  $2^{-Ct}$  using the respective SAL control value as the calibrator (equivalent to fold change over SAL controls). Data are shown as mean  $\pm$  SE with five mice in each group.  $*p < 0.05$  (versus corresponding WT value). *D*, Representative lung sections of day 21 BLM-/SAL-treated WT (SAL in *a*, BLM in *b*) and FIZZ2 KO mice (SAL in *c*, BLM in *d*) were stained with H&E for histological evaluation. Original magnification  $\times 100$ . *E*, Total BAL cell numbers were counted with a hemocytometer, and BAL differential cell analyses were conducted by flow cytometry at day 4 post-BLM injection. Data are shown as mean  $\pm$  SE with three mice in each group.  $*p < 0.05$ . *F*, Lung tissue CD3<sup>+</sup> T cells were analyzed by flow cytometry and data shown as mean  $\pm$  SE (three mice per group).  $*p < 0.05$ . *G*, Lung tissue samples were subjected to cDNA microarray analysis, and the results for select extracellular matrix relevant genes are shown. Data are shown as fold change over SAL-treated WT mice. Mean values are shown from three mice in each group. *H*, Lung fibroblasts from the indicated SAL- or BLM-treated strains of mice were analyzed for cell proliferation using the MTS dye. Results are shown as mean  $\pm$  SE with samples from three mice in each group.

**FIGURE 4.**

FIZZ2 induction of type I collagen and  $\alpha$ -SMA in MLFs. *A*, Normal MLFs were treated with the indicated doses of FIZZ2 for the indicated times and then analyzed for type I procollagen mRNA levels by qPCR. *B*, MLFs were treated with FIZZ2 (10 ng/ml) or TGF- $\beta$ 1 (0.1 ng/ml), or both as indicated, and then analyzed for type I procollagen mRNA by qPCR. For qPCR analysis, the GAPDH signal was used as internal control (reference) and the respective untreated controls (or “None”) as calibrator for the  $2^{-CT}$  calculations (equivalent to fold change over controls). Results are shown as mean  $\pm$  SE ( $n = 3$ ). \* $p < 0.05$

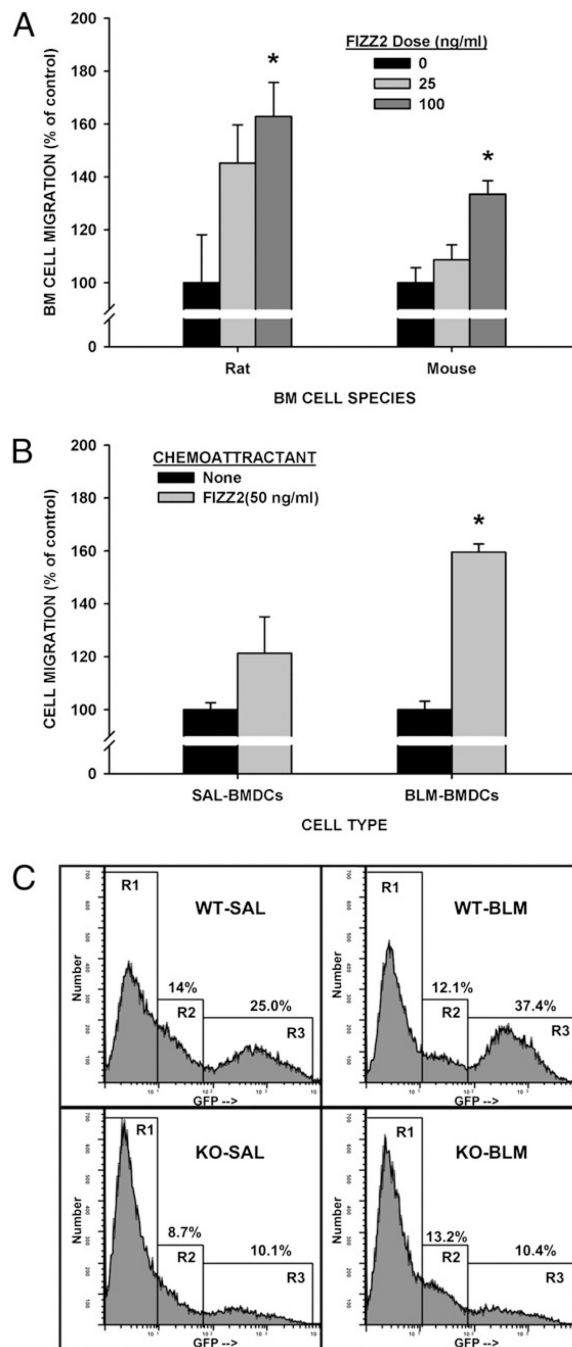


(compared with control in *A* and *B*, respectively). *C*, MLFs were treated with the indicated doses of FIZZ2 and then analyzed for  $\alpha$ -SMA protein levels by Western blotting. A representative Western blot is shown from three independent experiments with similar results.

**FIGURE 5.**

Effect of FIZZ2 on fibroblast proliferation. *A*, MLFs were treated with FIZZ2 at the indicated doses for 24 h, and cell proliferation was analyzed using MTS. Results are expressed as absorbance units and shown as mean  $\pm$  SE ( $n = 4$ ).  $*p < 0.05$  (versus untreated control). *B*, The cells were treated with or without FIZZ2 (10 ng/ml) for the indicated time points and then analyzed for phospho-ERK, phospho-AKT, phospho-JNK, and phospho-p38 expression by Western blotting. Representative blots are shown, which were repeated twice with comparable results. GAPDH protein was used as a loading control. *C*, Cells were

pretreated for 30 min with the MEK/ERK inhibitor PD98059 at 25 (“+”) or 50 (“++”) ng/ml and then treated with FIZZ2 (10 ng/ml) for 24 h as indicated. Cell proliferation was then analyzed using the MTS dye. Results are expressed in absorbance units and shown as mean  $\pm$  SE ( $n = 4$ ). \* $p < 0.05$  (versus cells treated with FIZZ2 only).

**FIGURE 6.**

FIZZ2 effects on BM cell migration. *A*, Fresh isolated whole BM cells from rats or mice were preloaded with fluorescent dye and then plated into 5- $\mu$ m inserts in 24-well Transwell plates. After 2 h of incubation with the indicated doses of FIZZ2 in the lower chambers, the cells that migrated to the lower chambers were quantitated by measuring the fluorescence with excitation and emission wavelengths of 494 and 517 nm, respectively. The results are normalized to the controls and expressed as percentages and shown as mean  $\pm$  SE ( $n = 3$ ). \* $p < 0.05$  (versus respective control values). *B*, Purified BMDCs from day 3 BLM-treated

(BLMBMDCs) or saline-treated (SAL-BMDCs) mice were similarly analyzed as in A for migration to medium only (“None”) or to 25 ng/ml FIZZ2 in the lower chambers. Results are expressed as in A.  $*p < 0.05$  (compared with the respective control value). C, BM cells from GFP transgenic mice were transplanted into WT control or FIZZ2 KO mice to create GFP-BM chimera mice of the respective recipient strain. After stable engraftment, the mice were treated with saline (WT-SAL or KO-SAL) or BLM (WT-BLM or KO-BLM) and 21 d later were analyzed for GFP expression in the lung adherent cell population by flow cytometry. Three populations were discerned corresponding with cells with undetectable (region R1), low (region R2), or high (region R3) GFP fluorescence.

**Table I**

Lung tissue FIZZ2 mRNA determinations by real-time PCR in rodent BLM-induced pulmonary fibrosis

Group (Total RNA)	BLM-Treated Group (Ct value, Mean $\pm$ SD)		PBS-Treated Group (Ct value, Mean $\pm$ SD)	
	FIZZ2	GAPDH	FIZZ2	GAPDH
Rat 1 wk <sup>a</sup> (100 ng)	36.09 $\pm$ 0.68	28.41 $\pm$ 0.08	ND	30.73 $\pm$ 0.50
Rat 2 wk (100 ng)	36.54 $\pm$ 0.59	23.81 $\pm$ 0.53	ND	24.44 $\pm$ 0.19
Mouse 1 wk (100 ng)	36.66 $\pm$ 0.61	23.91 $\pm$ 0.27	ND	24.48 $\pm$ 0.35
Mouse 1 wk (500ng)	35.32 $\pm$ 0.50	22.85 $\pm$ 0.17	ND	23.96 $\pm$ 0.14

<sup>a</sup>Refers to time point after BLM treatment.

ND, not detectable.

Table II

Selected gene expressions in BLM-/SAL-treated WT and FIZZ2 KO lung by microarray analysis (fold change over WT-SAL, shown as mean of three mice per group)

Gene Name	WT-SAL	WT-BLM	KO-SAL	KO-BLM	Gene Name	WT-SAL	WT-	KO-SAL	KO-BLM
MMP12	1.00	36.92	1.15	20.37	LmnB1	1.00	2.30	1.32	1.38
SAA3	1.00	31.42	0.94	1.91	FAP	1.00	2.25	1.04	0.92
Arg1	1.00	20.78	1.53	1.79	IL4Ra	1.00	2.20	1.14	1.15
TNC	1.00	16.46	0.97	3.85	Fzd1	1.00	2.19	1.18	1.32
TIMP1	1.00	16.10	0.76	1.89	Hey1	1.00	2.15	1.05	1.22
Sfrp1	1.00	13.62	1.41	2.73	TLR13	1.00	2.10	1.17	1.24
CCL8	1.00	11.29	1.15	3.42	Akt1	1.00	2.00	1.49	1.70
Thbs4	1.00	10.70	1.05	1.78	IL13Ra1	1.00	1.99	1.38	1.28
PLA1a	1.00	10.37	1.25	1.71	IL1	1.00	1.99	1.13	1.28
Eln	1.00	9.89	0.95	3.80	Fzd6	1.00	1.93	1.70	1.67
Lama	1.00	8.32	0.86	1.40	CTGF	1.00	1.92	0.82	1.10
Fh	1.00	7.90	0.99	1.79	Myosin	1.00	1.83	1.37	1.54
IGF1	1.00	7.16	0.95	2.42	Jak1	1.00	1.82	1.62	1.66
Col1a2	1.00	6.96	0.77	2.19	Casp3	1.00	1.77	1.07	1.30
CCL12	1.00	6.79	0.65	1.13	FGFR1	1.00	1.70	1.11	1.03
CCL9	1.00	6.75	1.58	2.80	PTEN	1.00	1.66	1.14	1.09
Frzb	1.00	6.06	1.06	1.06	Smad1	1.00	1.62	0.99	1.15
WISP1	1.00	6.05	0.77	1.67	TGFb1	1.00	1.60	1.09	1.30
Ube2c	1.00	5.46	0.69	1.65	CCL3	1.00	2.17	1.05	1.46
Col1a1	1.00	5.45	0.76	1.70	CCL5	1.00	0.43	1.14	0.81
CCR5	1.00	5.35	1.01	1.99	CAMK2b	1.00	1.11	0.16	0.27
CCR2	1.00	1.90	1.76	1.68	Nnt	1.00	0.84	0.33	0.39
CCR1	1.00	5.04	1.49	1.80	Dner	1.00	0.41	0.42	0.42
CCL2	1.00	4.60	0.96	1.15	MAP3K6	1.00	0.75	0.45	0.43
FIZZ1	1.00	4.02	0.79	0.63	Socs2	1.00	1.04	0.74	0.92
STOM	1.00	3.26	2.43	2.24	Ngdn	1.00	0.98	0.56	0.62
CTSE	1.00	3.14	0.89	0.92	FABP1	1.00	0.08	0.65	0.47

Gene Name	WT-SAL	WT-BLM	KO-SAL	KO-BLM	Gene Name	WT-SAL	WT-	KO-SAL	KO-BLM
E2F7	1.00	3.12	0.75	1.08	KLF15	1.00	0.29	0.68	0.48
CD86	1.00	3.04	1.14	2.04	MID1	1.00	1.52	7.52	7.25
BMP1	1.00	2.97	1.19	1.55	IL1b	1.00	1.04	2.90	1.71
Myc	1.00	2.58	1.03	1.23	Msn	1.00	2.47	1.93	2.10
Lypla3	1.00	2.52	1.50	1.92	Fos	1.00	1.60	3.13	1.53
Wnt5a	1.00	2.50	1.15	1.58	MUP1	1.00	2.05	4.72	1.36
Msn	1.00	2.47	1.93	2.10	NR4a1	1.00	0.93	2.75	2.17
Ube2t	1.00	2.44	0.87	1.24	Myc1	1.00	1.21	2.19	1.90
TLR2	1.00	2.38	1.18	1.61	STK17b	1.00	0.94	2.02	1.15
MMP2	1.00	2.31	0.63	1.86	FABP4	1.00	0.78	1.99	0.67

SAL, saline.



**Table III**Percentage of CD11c<sup>+</sup> lung cells in GFP-BM chimera mice

Experimental Group	GFP <sup>-</sup> (%) <sup>a</sup>	GFP <sup>+</sup> (%) <sup>a</sup>	GFP <sup>++</sup> (%) <sup>a</sup>
WT-SAL	6.96	85.50	90.54
WT-BLM	20.24	83.57	92.70
FIZZ2 KO-SAL	13.30	83.64	83.64
FIZZ2 KO-BLM	8.45	80.99	86.96

<sup>a</sup>GFP<sup>-</sup>, GFP<sup>+</sup>, and GFP<sup>++</sup> correspond with gating regions R1, R2, and R3, respectively, in Fig. 6C.

SAL, saline.